Research Article | Vol. 25, No. 19 | 18 Sep 2017 | OPTICS EXPRESS 22404

Optics EXPRESS

Mid-wave infrared beam steering based on high-efficiency liquid crystal diffractive waveplates

FANGWANG GOU, FENGLIN PENG, QITIAN RU, YUN-HAN LEE, HAIWEI CHEN, ZIQIAN HE, TAO ZHAN, KONSTANTIN L. VODOPYANOV, AND SHIN-TSON WU*

CREOL, The College of Optics and Photonics, University of Central Florida, Orlando, FL 32816, USA
**swu@ucf.edu*

Abstract: We demonstrated two liquid crystal diffractive waveplates: one optimized for near-infrared (1.06 μm), and another for mid-wave infrared (MWIR, 3~5 μm). By employing a low loss liquid crystal mixture UCF-M3, whose absorption loss is below 2% in the 4~5 μm spectral region, the grating achieves over 98% diffraction efficiency in a broad MWIR range. To switch the grating, both active and passive driving methods can be considered. In our experiment, we used a polymer-stabilized twisted nematic cell as the polarization rotator for passive driving. The obtained rise time is 0.2 ms and decay time is 10 ms.

OCIS codes: (050.1950) Diffraction gratings; (230.3720) Liquid-crystal devices; (230.2090) Electro-optical devices.

References and links

1. P. Werle, F. Slemr, K. Maurer, R. Kormann, R. Mücke, and B. Jänker, "Near-and mid-infrared laser-optical sensors for gas analysis," Opt. Lasers Eng. **37**(2-3), 101–114 (2002).
2. B. B. Lahiri, S. Bagavathiappan, T. Jayakumar, and J. Philip, "Medical applications of infrared thermography: a review," Infrared Phys. Technol. **55**(4), 221–235 (2012).
3. J. B. Carruthers and J. M. Kahn, "Angle diversity for nondirected wireless infrared communication," IEEE Trans. Commun. **48**(6), 960–969 (2000).
4. U. Willer, M. Saraji, A. Khorsandi, P. Geiser, and W. Schade, "Near- and mid-infrared laser monitoring of industrial processes, environment and security applications," Opt. Lasers Eng. **44**(7), 699–710 (2006).
5. B. D. Duncan, P. J. Bos, and V. Sergan, "Wide-angle achromatic prism beam steering for infrared countermeasure applications," Opt. Eng. **42**(4), 1038–1047 (2003).
6. R. Stanley, "Plasmonics in the mid-infrared," Nat. Photonics **6**(7), 409–411 (2012).
7. D. P. Resler, D. S. Hobbs, R. C. Sharp, L. J. Friedman, and T. A. Dorschner, "High-efficiency liquid-crystal optical phased-array beam steering," Opt. Lett. **21**(9), 689–691 (1996).
8. J. Kim, C. Oh, S. Serati, and M. J. Escuti, "Wide-angle, nonmechanical beam steering with high throughput utilizing polarization gratings," Appl. Opt. **50**(17), 2636–2639 (2011).
9. H. Sarkissian, S. V. Serak, N. V. Tabiryan, L. B. Glebov, V. Rotar, and B. Y. Zeldovich, "Polarization-controlled switching between diffraction orders in transverse-periodically aligned nematic liquid crystals," Opt. Lett. **31**(15), 2248–2250 (2006).
10. H. Chen, Y. Weng, D. Xu, N. V. Tabiryan, and S. T. Wu, "Beam steering for virtual/augmented reality displays with a cycloidal diffractive waveplate," Opt. Express **24**(7), 7287–7298 (2016).
11. E. Ouskova, D. Roberts, N. Tabiryan, D. M. Steeves, and B. R. Kimball, "Diffractive waveplates for long wave infrared," Proc. SPIE **10194**, 1019404 (2017).
12. H. Sarkissian, B. Park, N. Tabirian, and B. Zeldovich, "Periodically aligned liquid crystal: potential application for projection displays," Mol. Cryst. Liq. Cryst. (Phila. Pa.) **451**(1), 1–19 (2006).
13. S. R. Nersisyan, N. V. Tabiryan, D. M. Steeves, and B. Kimball, "Optical axis gratings in liquid crystals and their use for polarization insensitive optical switching," J. Nonlinear Opt. Phys. Mater. **18**(1), 1–47 (2009).
14. F. Peng, H. Chen, S. Tripathi, R. J. Twieg, and S. T. Wu, "Fast-response infrared phase modulator based on polymer network liquid crystal," Opt. Mater. Express **5**(2), 265–273 (2015).
15. N. V. Tabiryan, S. R. Nersisyan, D. M. Steeves, and B. R. Kimball, "The promise of diffractive waveplates," Opt. Photonics News **21**, 41–45 (2010).
16. H. Xianyu, S. T. Wu, and C. L. Lin, "Dual frequency liquid crystals: a review," Liq. Cryst. **36**(6–7), 717–726 (2009).
17. S. Gauza, X. Zhu, W. Piecek, R. Dabrowski, and S. T. Wu, "Fast switching liquid crystals for color-sequential LCDs," J. Disp. Technol. **3**(3), 250–252 (2007).

#303754 https://doi.org/10.1364/OE.25.022404
Journal © 2017 Received 31 Jul 2017; revised 22 Aug 2017; accepted 26 Aug 2017; published 6 Sep 2017

Optics EXPRESS

18. H. Chen, M. Hu, F. Peng, J. Li, Z. An, and S. T. Wu, "Ultra-low viscosity liquid crystal materials," Opt. Mater. Express **5**(3), 655–660 (2015).
19. F. Peng, Y. Chen, S.-T. Wu, S. Tripathi, and R. J. Twieg, "Low loss liquid crystals for infrared applications," Liq. Cryst. **41**(11), 1545–1552 (2014).
20. M. Schadt and W. Helfrich, "Voltage-dependent optical activity of a twisted nematic liquid crystal," Appl. Phys. Lett. **18**(4), 127–128 (1971).
21. Y. Q. Lu, F. Du, Y. H. Lin, and S. T. Wu, "Variable optical attenuator based on polymer stabilized twisted nematic liquid crystal," Opt. Express **12**(7), 1221–1227 (2004).
22. C. H. Gooch and H. A. Tarry, "The optical properties of twisted nematic liquid crystal structures with twisted angles ≤ 90°," J. Phys. D. **8**(13), 1575–1584 (1975).
23. J. Sun and S. T. Wu, "Recent advances in polymer network liquid crystal spatial light modulators," J. Polym. Sci., Part B, Polym. Phys. **52**(3), 183–192 (2014).
24. L. Hu, D. S. Hecht, and G. Grüner, "Infrared transparent carbon nanotube thin films," Appl. Phys. Lett. **94**(8), 081103 (2009).
25. Z. Wu, Z. Chen, X. Du, J. M. Logan, J. Sippel, M. Nikolou, K. Kamaras, J. R. Reynolds, D. B. Tanner, A. F. Hebard, and A. G. Rinzler, "Transparent, conductive carbon nanotube films," Science **305**(5688), 1273–1276 (2004).

1. Introduction

Mid-wave infrared (MWIR), which spans the 3–5 μm wavelength range, is a spectral region of great interest in materials analysis, chemical and biomolecular sensing, communication systems, and security inspections, just to name a few [1–4]. Therefore, the development of MWIR optical and photonic devices such as laser sources, phase modulators and polarization controllers are in high demand. Particularly, for space-based applications, a high efficiency, large angle and high accuracy optical beam steering device is required. Several strategies have been proposed to steer a MWIR laser beam, including arrays of prisms [5], plasmonic devices [6], and nematic liquid crystal (LC) optical phased array [7]. Each technology has its own pros and cons. For example, Risley prism can achieve a wide beam steering range, however, it is often bulky and expensive, especially in the MWIR. Plasmonic device is able to control the divergence and direction of diffracted beams by small apertures, but it is challenging to develop this technique into cost-effective, compact and reliable systems. For the nematic LC optical phased array, it deflects the beam with high efficiency, high accuracy and fast response time, but its deflection angle is relatively small.

Non-mechanical beam control devices based on LC cycloidal diffractive waveplate (CDW) have been demonstrated to achieve high efficiency, wide angle and large aperture [8–11]. It consists of a thin LC layer, wherein the LC optical axis rotates continually along a Cartesian axis. If the incident light is circularly polarized, then the + 1st or −1st diffraction order would appear depending on the input polarization. Previous efforts have mainly focused on deflecting a laser beam in the visible, near infrared, short-wavelength infrared (SWIR) or long IR regions, yet little work in MWIR has been investigated. The major challenge is the relatively large absorption loss of LC material in this region.

In this paper, we demonstrate two high efficiency (>98%) liquid crystal diffractive waveplates for laser beam steering: one optimized at near IR and another at MWIR. The employed LC material UCF-M3 has an absorption loss less than 2% in the λ = 4~5 μm region, which contributes to the high efficiency. To switch the grating, both active and passive driving methods can be considered. For passive driving, we used a polarization rotator consisting of a polymer-stabilized twisted nematic (TN) LC cell and a quarter-wave ($\lambda/4$) plate. The obtained rise time 0.2 ms and decay time is 10 ms.

2. Experiment and results

2.1 Device structure

Figure 1 depicts the device structure of the CDW we employed. The LC director distribution is homogeneous along z axis, while varying continually with a pitch Λ in x-y plane, as described by:

Optics EXPRESS

$$\vec{n}(x) = [\cos(qx), \sin(qx)], q = 2\pi / \Lambda. \quad (1)$$

The properties of this grating are modulated with period $\Lambda/2$ because the LC directors are indistinguishable in the + $\vec{n}$ and – $\vec{n}$ directions. The grating thickness d and LC birefringence Δn are chosen to satisfy the half-wave phase retardation condition $d\Delta n = \lambda/2$, where λ is the free space wavelength.

Base on the grating pitch Λ, the wavelength dependent diffraction angle θ can be described as follows:

$$\theta = \sin^{-1}(2\lambda / \Lambda), \quad (2)$$

From Eq. (2), for a given wavelength a smaller pitch length would lead to a larger diffraction angle. It is also noteworthy that the grating only has three orders (0th and ± 1st orders), and theoretically 100% diffraction efficiency into one of the first-orders is possible when $d\Delta n = \lambda/2$ and input light is circularly polarized [12].

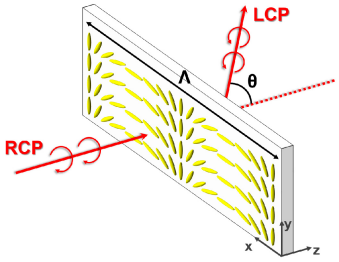

Fig. 1. Schematic structure of the cycloidal diffractive waveplate. Λ is the grating pitch length. Through the grating, the incident right-handed circular polarized (RCP) light is converted to + 1st order left-handed circular polarized (LCP) output.

To fabricate such a grating [13], we first coated a thin layer of photo-alignment material brilliant yellow on glass or sapphire substrates, and then assembled LC cell with a desired cell gap, depending on the operation wavelength. Afterwards, the cell was exposed by two interfering coherent laser beams with orthogonal circular polarizations. The effective polarization of the interference beams is linear and rotating in a cycloidal manner. Thus, the LC directors are oriented by the photoalignment pattern [Fig. 1]. To minimize the absorption loss in MWIR region, we prepared a LC mixture (UCF-M3) with $\Delta n = 0.262$ at $\lambda = 3\sim5$ μm [14], and the grating thickness was adjusted to satisfy the half-wave condition for the intended wavelength. By controlling the angle between two laser beams, we can tune the pitch Λ. Figure 2(a) shows the image of our fabricated grating under a polarizing optical microscope. The grating pitch $\Lambda = 61.73$ μm. Because $\Lambda >> \lambda$, we can expand Eq. (2) and find that diffraction angle is linearly proportional to λ. To validate this relation, we measured the diffraction angle at various laser wavelengths. Results are shown in Fig. 2(b). Good agreement between simulation and experiment is obtained. At $\lambda = 4$ μm, the diffraction angle is $\theta = 7.6°$.

Optics EXPRESS

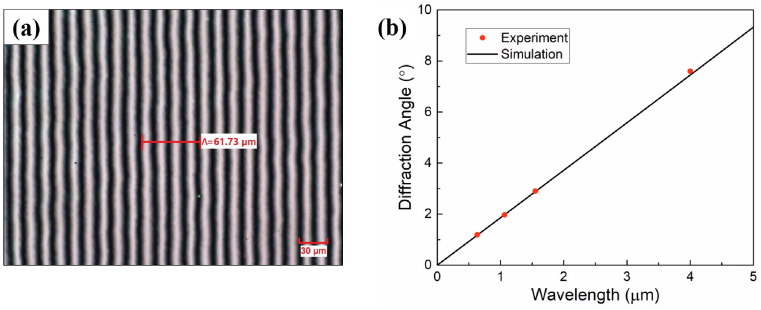

Fig. 2. (a) The image of a cycloidal diffractive waveplate under polarizing optical microscope. (b) Diffraction angle as a function of wavelength: Dots are measured data and line is calculated from Eq. (2).

2.2 Near IR

The diffraction efficiency could be calculated using following simplified equation based on Jones matrix approach [13, 15]:

$$\eta(\lambda) = \sin^2(\frac{\pi d \Delta n}{\lambda}). \tag{3}$$

The simulation results agree well with experiment (red dots), as Fig. 3 shows. At λ = 1.06 μm (Δn = 0.278), to satisfy $d\Delta n = \lambda/2$ the grating thickness should be d = 1.91 μm. However, in experiment our cell gap is 2.07μm, so that the diffraction efficiency is 98%. This device also exhibits a high diffraction efficiency at λ = 0.514 μm. From Fig. 3, we also notice that the diffraction efficiency is more sensitive to the wavelength in the visible than in the near-IR and SWIR regions, indicating that it is possible to achieve high diffraction efficiency in a broad MWIR range. We will prove this later.

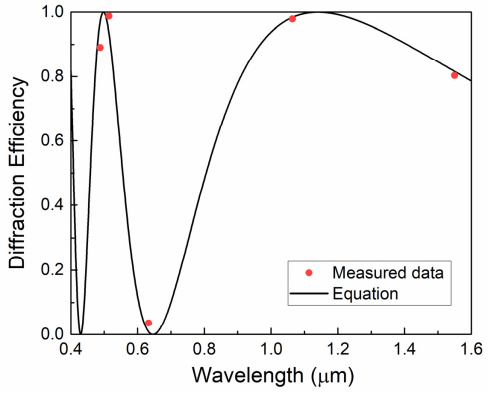

Fig. 3. Wavelength dependent diffraction efficiency with d = 2.07 μm. Dots are measured data and line is calculated result using Eq. (3).

Two driving schemes can be utilized to switch such a grating [15]: active or passive driving. For active driving, the grating consists of LC material with electrodes on both substrates. The voltage is applied directly on the grating to switch the LC directors between spatially patterned waveplate and homeotropic state. As a result, the grating could select between + 1st order (or −1st order, depending on the polarization of input light) and 0th order. For passive driving, we use a polarization rotator to select the input polarization between LCP and RCP in order to switch between + 1st and −1st order. In this case, the grating is

Optics EXPRESS

commonly made of LC polymer film which cannot be activated by an electric field. Therefore, the film thickness must be well-controlled to obtain a high diffraction efficiency.

Figure 4(a) depicts the measured response time for active driving, and the inset figure shows the driving scheme. With 10 V_{rms} of applied voltage (1 kHz), the rise time is 7 ms and decay time is 61 ms. To shorten response time, we can also use a dual-frequency liquid crystal (DFLC) mixture [16]. The advantage is that both fast rise time and decay time can be achieved. Another approach is to use a higher Δn yet low viscosity LC material [17, 18]. For example, by using the mixture LC-1 described in [17], the grating thickness can be reduced to 1.61 μm and submillisecond response time can be achieved. However, this mixture contains isothiocyanato (NCS) polar group, which has a broad and strong absorption band in the 4.5–5.2 μm region [19]. In order to extend the application of the grating to MWIR, LC materials with low absorption are required.

For passive driving [the inset of Fig. 4(b)], a polymer-stabilized TN (PSTN) cell in combination with a quarter-wave plate (QWP) is used as broadband switchable polarization rotator [20, 21], which controls either RCP or LCP to enter the grating. To fabricate the PSTN cell, we doped 5 wt% monomer RM257 and 0.2 wt% photo-initiator into LC host UCF-M3. The precursor was injected into a 3.6-μm TN cell, which satisfies the Gooch-Tarry first minimum condition $d\Delta n = \sqrt{3}\lambda/2$ at λ = 1.06 μm [22]. The sample was exposed to UV light (λ = 385 nm, intensity 220 mW/cm^2) for 1 hour, to form polymer network. These polymer networks provide a strong anchoring energy, which helps improve the response time, but the tradeoff is increased driving voltage [14, 23]. The required operation voltage of the PSTN cell is 80 V_{rms}, and the measured rise time is 0.2 ms and decay time is 10 ms. The scattering loss of such a TN cell is 3% at V = 0 and 9% at 80V. However, in the MWIR region the scattering loss should be negligible because the domain size is much smaller than the wavelength.

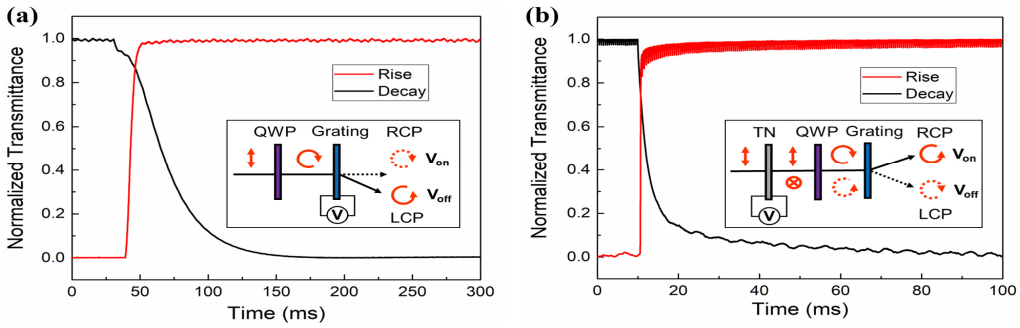

Fig. 4. Measured rise and decay time with (a) active and (b) passive driving. The inset figures show driving schemes. For active driving, the applied voltage is 10 V_{rms}. For passive driving, a PSTN cell is used as the polarization rotator, and the applied voltage is 80 V_{rms}. λ = 1.06 μm.

2.3 MWIR

For our MWIR measurements, we built an optical parametric oscillator (OPO) tunable in the 3-5 μm range. The OPO was based on periodically poled lithium niobate (PPLN) crystal and was pumped by a diode-pumped Nd:YAG laser (λ = 1.06 μm). As shown in Fig. 5, the OPO was formed by two flat dichroic mirrors (M1 and M2), which were highly reflective at the OPO 'signal' wave (1.35-1.65 μm) and highly transmissive at the 'idler' wave (3-5 μm). The 20-mm-long PPLN crystal was kept at T = 50 °C and had a ‘fanned’ grating with a quasi-phase-matched (QPM) period that varied from 25.8 μm to 31.5 μm across the width of the crystal. The wavelength of the idler wave could be tuned anywhere in the range from 3 to 5 μm by linearly moving the PPLN crystal across the beam, with pulse energy 100 μJ (average power 10 mW) at λ = 3 μm and 10 μJ at λ = 5 μm. The OPO beam was close to diffraction limited. A 45° dichroic mirror was used to reject the 1.06-μm pump and signal waves. Additionally, a long pass filter (> 3 μm) was used to select only the idler wavelength.

Optics EXPRESS

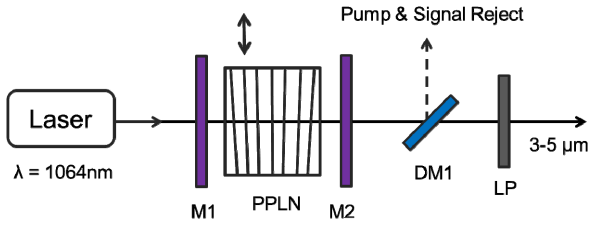

Fig. 5. PPLN OPO setup. M1, M2: OPO dichroic mirrors; DM1: dichroic mirror for pump and signal rejection; LP: 3-μm long pass filter.

In order to minimize the absorption of MWIR, we use sapphire instead of glass as the grating substrate. Figure 6(a) depicts the transmittance spectrum of UCF-M3 measured by FTIR (Perkin Elmer Spectrum One FTIR Spectrometer) at room temperature with an unpolarized light. The cell gap is d = 9 μm. Although a narrow absorption peak appears at λ = 4.45μm due to CN vibration, in the λ = 4~5 μm region the baseline transmittance is over 98%. Figure 6(b) shows the measured grating diffraction efficiency as a function of wavelength. As expected, this device exhibits a high diffraction efficiency (>98%) over a broad MWIR range from 4 to 5 μm. To switch the grating, we can coat carbon nanotube or graphene [24, 25] on the sapphire substrate as the electrode. In the MWIR, Δn is reduced to 0.262 and a larger grating thickness is required to satisfy the half-wave phase retardation condition. In our experiment, the grating thickness is d = 8.51 μm. For active driving, because the LC response time is proportional to d^2, the decay time is estimated to be ~1s, which is 17x slower than that at λ = 1.06 μm. To shorten response time, passive driving with a polymer-stabilized TN LC is preferred. This is because the response time of a polymer-stabilized TN LC is not determined by the cell gap but by the domain size, which is governed by the polymer concentration and curing condition [23]. If we keep the same polymer concentration, then the response time for the MWIR device would be comparable to that at λ = 1.06 μm. However, the required TN cell gap for λ = 4 μm is about 4x thicker than that at λ = 1.06 μm. Thus, the required driving voltage would increase by ~4x, i.e. ~320V_{rms}. This problem can be mitigated by reducing the polymer concentration, i.e. increasing the domain size. In the MWIR, light scattering caused by the increased domain size is more forgiven, but the tradeoff is slower response time.

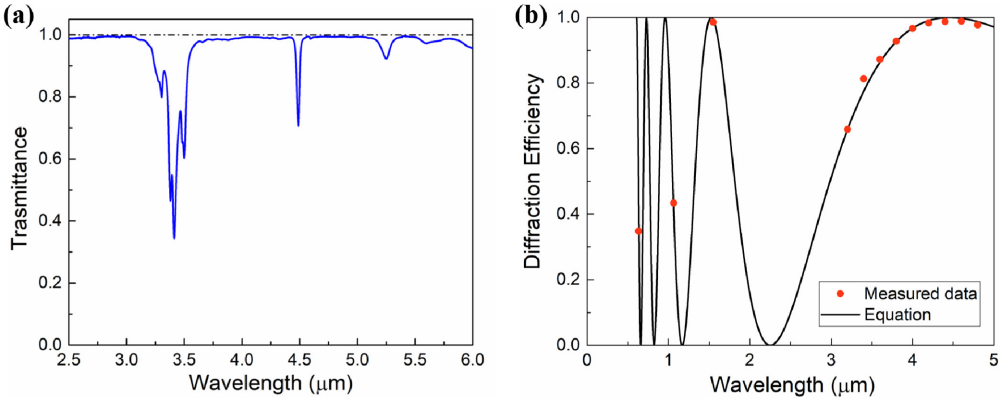

Fig. 6. (a) Measured transmittance spectrum of UCF-M3 in the MWIR region with cell gap d = 9 μm. (b) Wavelength dependent diffraction efficiency. d = 8.51μm. Dots are measured data and line is calculated result using Eq. (3).

3. Conclusion

We have demonstrated liquid crystal diffractive waveplates in the near IR and MWIR regions. With low absorption liquid crystal mixture UCF-M3, the device could achieve over 98%

Optics EXPRESS

diffraction efficiency in a broad MWIR region. To switch the grating, the active driving method is to apply voltage directly to the grating. Using this method, at 10V we obtained 7-ms rise time and 61-ms decay time. To shorten response time, we used passive driving with a polymer-stabilized twisted nematic LC as a polarization rotator, and obtained 0.2 ms rise time and 10 ms decay time. However, the required operation voltage is increased to 80 V_{rms}.

Funding

Air Force Office of Scientific Research (AFOSR) (FA9550-14-1-0279).

Acknowledgments

The authors would like to thank AFOSR for financial support.